An Antagonist of Dishevelled Protein-Protein Interaction Suppresses β-Catenin–Dependent Tumor Cell Growth

Naoaki Fujii,[1,3] Liang You,[3] Zhidong Xu,[3] Kazutsugu Uematsu,[8] Jufang Shan,[5,7] Biao He,[3] Iwao Mikami,[3] Lillian R. Edmondson,[4] Geoffrey Neale,[6] Jie Zheng,[5,7] R. Kiplin Guy,[1,2] and David M. Jablons[3]

Departments of [1]Pharmaceutical Chemistry and [2]Cellular and Molecular Pharmacology; [3]Thoracic Oncology Laboratory, Department of Surgery; and [4]Genome Analysis Core, Cancer Center, University of California San Francisco, San Francisco, California; [5]Department of Structural Biology and [6]Hartwell Center for Bioinformatics and Biotechnology, St. Jude Children's Research Hospital; [7]Department of Molecular Sciences, University of Tennessee Health Science Center, Memphis, Tennessee; and [8]Division of Medical Oncology, Tokai University School of Medicine, Isehara, Japan

Abstract

Recent progress in the development of inhibitors of protein-protein interactions has opened the door for developing drugs that act by novel and selective mechanisms. Building on that work, we designed a small-molecule inhibitor of the Wnt signaling pathway, which is aberrantly activated across a wide range of human tumors. The compound, named FJ9, disrupts the interaction between the Frizzled-7 Wnt receptor and the PDZ domain of Dishevelled, down-regulating canonical Wnt signaling and suppressing tumor cell growth. The antitumorigenic effects of FJ9 were pronounced, including induction of apoptosis in human cancer cell lines and tumor growth inhibition in a mouse xenograft model. FJ9 is thus among the first non-peptide inhibitors to show therapeutic efficacy through disruption of PDZ protein-protein interactions. [Cancer Res 2007;67(2):573–9]

Introduction

Aberrant activation of the Wnt signaling pathway is implicated in the development of a broad spectrum of tumors (1–3). Up-regulation of Wnt-associated genes has been shown to play a role in the development of human cancers. For example, Wnt16 is overexpressed in the pre-B subtype of acute lymphoblastic leukemia, which is characterized by a t(1;19) chromosomal translocation that results in the E2A-PBX1 fusion protein. *Wnt16*, a target gene of E2A-PBX1, plays key a role in leukemogenesis in such cases (4, 5). However, although many Wnt genes (*Wnt1, Wnt3a*, and *Wnt16*) are thought to have oncogenic potential, others (*Wnt5a* and *Wnt7a*) have the characteristics of tumor suppressor genes (2). For example, most lung cancer cell lines and tissues show loss of Wnt7a, and the restoration of Wnt7a expression up-regulates E-cadherin and inhibits proliferation of non–small cell lung cancer cells in a peroxisome proliferator-activated receptor γ–dependent manner (6–8). Loss of expression of β-catenin and E-cadherin is considered a marker of poor prognosis for lung cancer patients (9–12). Taken together, the evidence suggests that Wnt pathway activation may have opposing functions that depend on the specific ligand/receptor combination. Because of the multiple functions of the Wnt family, inhibition of all Wnt signaling may not be a perfect strategy for tumor therapy. One solution would be to target only Wnt signaling molecules that contribute significantly to tumorigenesis.

A promising way to investigate the role of specific Wnt molecules in tumorigenesis is to observe whether inhibition of their signaling causes tumor promotion or suppression. For example, we have shown that silencing of the *Wnt16* and *Wnt1* genes suppressed the growth of pre-B leukemia cells and lung cancer cells, respectively (4, 13). Small-molecule drugs that inhibit Wnt signaling can be used to test our hypothesis that Wnt signaling promote the growth of lung cancers. Such drugs can be rationally designed by targeting the Frizzled (Frz) family of Wnt receptors, which relay Wnt signaling to the β-catenin/Tcf pathway (14).

Several observations suggest that different Wnt molecules use a different subtypes of Frz receptor. For example, Wnt7a relays signal via Frz5 (15) and Frz9 (8). On the other hand, Wnt signaling via Frz7 is reported to have oncogenic potential (16). Frz7 ectodomain (an antagonist form) expression inhibits tumor growth in a colon cancer cell line (17), and Frz7 is overexpressed in tumor cell lines (18) and tumor tissues (19). Therefore, we hypothesized that selective targeting of Frz7 will suppress oncogenic Wnt signaling without interfering with tumor-suppressive Wnt7a signaling. Frz7 interacts directly with a PDZ protein interaction domain of the Dishevelled (DVL) family (20). DVL3 is overexpressed in a wide spectrum of cancer cells (21). Wnt signaling in the β-catenin pathways seems to be induced by DVL overexpression (22, 23). Therefore, disrupting the Frz7-DVL protein-protein interaction (24) represents a promising strategy for cancer therapy. Previously, we have shown that dominant-negative DVL lacking the PDZ domain decreased cytosolic β-catenin levels, diminished Tcf-mediated transcription, and suppressed tumorigenesis of mesothelioma cells *in vitro* and *in vivo* (22). This study suggests that the PDZ domain of DVL represents an attractive cancer therapeutic target.

The PDZ domain is a common protein-protein interaction module that recognizes short peptide motifs on the COOH termini or internal sequences that structurally mimic a sharp β-turn structure of the cognate ligand (25). PDZ domains mediate crucial protein-protein interactions that enforce localization and organization of proteins in a variety of submembranous complexes associated with cell signal mediators, including ion channels, transmembrane receptors, and regulatory enzymes (26). The therapeutic usefulness of PDZ protein-protein interaction

Note: Supplementary data for this article are available at Cancer Research Online (http://cancerres.aacrjournals.org/).

N. Fujii and L. You contributed equally to this work.

Current address for N. Fujii and R.K. Guy: Department of Chemical Biology and Therapeutics, St. Jude Children's Research Hospital, Memphis, TN 38105.

Requests for reprints: Naoaki Fujii, Department of Chemical Biology and Therapeutics, St. Jude Children's Research Hospital, M/S1000, 332 North Lauderdale Street, Memphis, TN 38105. Phone: 901-495-5854; Fax: 901-495-5715; E-mail: Naoaki.Fujii@stjude.org.

doi:10.1158/0008-5472.CAN-06-2726

antagonism has been clearly shown by using a peptide antagonist (ref. 27; reviewed in ref. 28). Regardless, few efforts have been made to design specific non-peptide antagonists of PDZ domain interaction. Our aim in this study was to design a proof-of-principle small-molecule inhibitor to block the interaction between the PDZ domain of DVL and the COOH-terminal region of Frz receptor and to test whether it inhibits down-stream Wnt signaling and suppresses cancer cell growth. We reported the structure-based design of an indole-3-carbinol compound that mimics the tetrapeptide sequence binding to a PDZ domain (29). This compound formed a covalent adduct by electrophilic alkylation of a histidine residue in the PDZ domain and therefore had limited therapeutic potential because electrophilic inhibitors often lack specificity in targeting biomolecules. To overcome this, we designed a new non-electrophilic indole-2-carbinol–based chemical scaffold. One compound from this series inhibits the protein-protein interaction between the DVL PDZ domain and Frz7. That inhibitor, named FJ9, markedly down-regulates canonical Wnt signaling and suppresses tumor growth.

Materials and Methods

Cell lines. Human tumor cell lines (NCI-H1703, NCI-H460, NCI-A549, NCI-H28, HCT116 $p53^{-/-}$, HeLa, LOX, and HEK293T) were obtained from the American Type Culture Collection (Manassas, VA). These cells were cultured in RPMI 1640 (NCI-H1703, NCI-H460, NCI-A549, NCI-H28, HeLa, LOX, and HCT116 $p53^{-/-}$), Eagle MEM (HeLa), or DME H-21 high-glucose (HEK293T) media supplemented with 10% fetal bovine serum, penicillin (100 IU/mL), and streptomycin (100 mg/mL). Normal human small airway epithelial cells (SAEC) and normal human bronchial epithelial (NHBE) cells were obtained from Clonetics (Walkersville, MD) and cultured using the Clonetics SAGM Bullet kit. LP9 was purchased from the Cell Culture Core at Brigham and Women's Hospital (Rheinwald Lab, Boston, MA) and immortalized by introduction of *hTERT* as described (30). To obtain LP9 cell line expressing wild-type DVL, the *Xho*I/*Eco*RI mouse DVL1 (mDVL1) fragment of the pCS-mDVL1 was cloned into the *Xho*I/*Eco*RI site of pLXN. In the same manner, pLXN-mΔPDZ-DVL1 was constructed from pCS-mΔPDZ-DVL1. To prepare retroviral stocks, Phoenix A cells were transfected with pLXN-neo-DVL1, ΔPDZ-DVL1, or pLXN-neo (empty vector) using LipofectAMINE Plus reagent. Retroviral constructs were introduced into LP9-TERT and selected after culture in neomycin (50 μg/mL, 7 days). The LP9 cells were cultured in M199 medium containing 15% calf serum (Hyclone, Logan, UT) plus 10 ng/mL epidermal growth factor and 0.4 μg/mL hydrocortisone. All cells were maintained at 37°C in a humid incubator with 5% CO_2.

Antibodies. Anti-β-catenin antibody was purchased from Transduction Laboratories (Lexington, KY). Anti–cyclin D1, anti-c-*myc*, and anti-survivin antibodies were from Santa Cruz Biotechnology (Santa Cruz, CA). Anti-β-actin, anti–phospho-473 Akt, and anti–phospho-c-jun (Ser^{63}) antibody were from Cell Signaling Technology, Inc. (Beverly, MA). Anti–phospho-c-Jun NH_2-terminal kinase (anti–phospho-JNK; Thr^{183}/Tyr^{185}) antibody was from Promega, Inc. (Madison, WI).

Plasmids. myc-Human Frz7-pcDNA3. The total mRNA sample of SW480 colon cancer cells was reverse transcribed by using SuperScript II RnaseH-Reverse Transcriptase (Invitrogen, Carlsbad, CA) according to the manufacturer's protocol. The coding region of the human Frz7 (hFrz7) in the obtained cDNA sample was amplified by a standard PCR protocol using 5′-TATAGCTAGCCACCATGGAACAAAAACTTATTTCTGAAGAAGATCT-GATGCGGGACCCCGGCGCGGCC-3′ as a forward primer and 5′-TATAAA-GCTTTTATCATACCGCAGTCTCCCCCTTGCT-3′ as a reverse primer. The PCR product was purified by agarose-gel electrophoresis, digested by *Nhe*II and *Hin*dIII, and inserted into pcDNA3 vector (Invitrogen) by T4 DNA Quick ligation kit (New England Biolabs, Beverly, MA). The positive clone was identified by sequencing of the isolated plasmids from the transformed DH5 α cells [University of California, San Francisco (UCSF) sequencing facility]. Hemagglutinin (HA)–negative mDVL1-$pCS2^+$ and ΔPDZ-DVL1 were described previously (22).

Protein expression. The coding region of the PDZ domain of the human DVL3 was amplified by a standard PCR protocol using 5′-CCTTAAG-GATCCCTCAACATCATCACGGTCAC-3′ as a forward primer, 5′-CCTTAA-CTCGAGTCTATGGGTCCCAGCACTTGGCTA-3′ as a reverse primer and the human DVL3 full-length cDNA as a template. The PCR product was purified by agarose-gel electrophoresis, digested by *Bam*HI and *Xho*I, and inserted into pGEX-6P2 vector (Amersham, Arlington Heights, IL) by T4 DNA ligase to prepare human DVL3 (hDVL3) PDZ-pGEX-6P2. The DVL PDZ-pGEX-6P2 vector was transformed into BL21 (DE3) cells, and clones were selected by a standard protocol. The positive clones were identified by sequencing of the maintained plasmids (UCSF sequencing facility). The cells were treated by isopropyl-L-thio-B-D-galactopyranoside for inducing the glutathione *S*-transferase (GST) fusion protein expression, grown in Luria-Bertani culture media at 20°C overnight, and lysed by sonication. The GST-hDVL3 PDZ domain protein was purified by glutathione-Sepharose 4B (Amersham) from the crude lysate, analyzed by SDS-PAGE, and quantified by a standard BCA assay (Pierce, Rockford, IL). GST-hDVL1 PDZ domain protein was prepared in a similar manner.

Compound preparation. FJ9 was synthesized as shown in Supplementary Fig. S1 and stored as a 30 to 50 mmol/L aqueous solution (containing no DMSO) of the monosodium salt.

AlphaScreen energy transfer assay. Serial dilutions of FJ9 (0.1–1,000 μmol/L) were made in the AlphaScreen GST-binding buffer supplemented with biotin-GKLQSWRRF peptide (10 μmol/L) and the GST-DVL1 or GST-DVL3 PDZ domain (100 nmol/L). The biotin-GKLQSWRRF peptide was not added in a concurrent control experiment. Each sample solution was plated in a 384-well plate in triplicate. To each well, 5 μL of anti-GST acceptor beads (Perkin-Elmer, Wellesley, MA) was added. After incubation at room temperature for 30 min in the dark, 5 μL of streptavidin donor beads (Perkin-Elmer) was added. After further incubation at room temperature for 60 min in the dark, signal was read with an EnVision (Perkin-Elmer) plate reader by the standard AlphaScreen method. Each result is reported as the mean and SD. Binding curves were fitted, and the K_i values were calculated by using Prism software (GraphPad, San Diego, CA).

Coimmunoprecipitation. HEK293T cells were transfected in six-well plates with 4 μg of HA-mDVL1-$pCS2^+$ and myc-hFrz7-pcDNA3 by using FuGENE6 (Roche, Indianapolis, IN) according to the manufacturer's recommendation for 20 h. The medium was replaced with fresh medium containing 0, 100, or 300 μmol/L FJ9, and the cells were incubated for an additional 24 h. The cells were washed once with PBS and lysed by using a Mem-PER kit (Pierce). The lysates were diluted with M-PER buffer (Pierce) and immunoprecipitated by using an anti-HA immunoprecipitation kit (3 μL of anti-HA agarose; Pierce) according to the manufacturer's protocol. The precipitates and whole lysate samples (transfection control) were analyzed by Western blot.

$^1H/^{15}N$ heteronuclear single-quantum coherence nuclear magnetic resonance. Chemical shift measurements were done with a Varian INOVA 600 MHz nuclear magnetic resonance (NMR) spectrometer at 25°C. ^{15}N-labeled mDVL1 PDZ domain (0.3 mmol/L) was buffered in 100 mmol/L potassium phosphate (pH 7.5), 10% D_2O, 0.5 mmol/L EDTA, and 1 mmol/L DTT. A 50 mmol/L solution of FJ9 monosodium salt in water (pH 7.5) was added directly to the PDZ domain solution. A series of titration were carried out. The protein/ligand ratio was 1:0.5, 1:1, 1:2, 1:3, 1:5, and 1:10.

Tcf reporter assay. Cells were plated in six-well plates and transfected with the TOPflash or FOPflash reporter plasmid (Upstate, Lake Placid, NY) as described (22). After incubation for 24 h, FJ9 was added. Each reporter gene transcript was normalized to the luciferase activity of the pRL-TK reporter (cotransfected internal control). The Dual-Glo Luciferase Assay kit (Promega) was used according to the manufacturer's protocol. All experiments were done independently in triplicate. The results reported are the means and SDs normalized to the TOPflash/pRL-TK reporter activity in the absence of FJ9.

Western blot. The cells (six-well plate) were treated with the FJ9 for 24 to 48 h, washed by PBS, and lysed with M-PER mammalian cell lysis buffer (Pierce) supplemented with Complete protease inhibitor cocktail (Roche) and phosphatase inhibitor cocktail SetII (Calbiochem, La Jolla, CA).

To normalize the PAGE loading, the protein concentration of each crude lysate was determined by BCA assay (Pierce) according to the manufacturer's protocol. The normalized amounts of the lysate samples were loaded on SDS-PAGE (10% or 12% ReadyGel; Bio-Rad, Richmond, CA) and transferred to the polyvinylidene difluoride or nitrocellulose membranes. For detecting alterations of β-catenin, cytosolic extracts were prepared and examined as described previously (31). β-Actin served as loading control.

DVL small interfering RNA transfection was carried out as described previously (23). HCT116 cells were plated 24 h before treatment in six-well plates at a density of 1.5×10^6 per well in RPMI 1640 supplemented with 10% FCS without antibiotics. Cells were transfected with siRNAs (100 nmol/L) using oligofectamine (Invitrogen) and incubated for 72 to 96 h. Transfected cells were collected to extract protein for RNA isolation for reverse transcription-PCR (RT-PCR) analysis.

Taqman RT-PCR was carried out as shown in the Supplementary Information.

Analysis of apoptosis. Cells in six-well plates were treated with FJ9 in the culture medium for 3 to 6 days, treated with trypsin, stained with Annexin V-FITC (Apoptosis Detection kit; Oncogene, Uniondale, NY) according to the manufacturer's protocol, and immediately analyzed by flow cytometry (FACScan; Becton Dickinson, Franklin Lake, NJ) as described previously (32). Cytometry was recorded in two dimensions: the *x*-axis represented Annexin V-FITC staining, and the *y*-axis represented propidium iodide staining. Percent apoptosis was calculated as the percentage of FITC-positive cells (sum of *top right* and *bottom right* areas of the graph).

***In vivo* tumor suppression study.** Groups of eight 6-week-old female nude mice (strain: NSWNU-M; Taconic, Germantown, NY) were injected s.c. in the dorsal area with four million H460 tumor cells in 100 μL PBS. After 7 days, during which the tumors developed essentially uniformly, the animals began receiving daily i.p. injections of FJ9 (50 mg/kg in 80 μL PBS) or of 80 μL PBS (days 8–21 after cell injection). Tumor size and body weight were measured on days 12, 14, and 16 after the start of FJ9 treatment. Mice that did not form tumors or that died of causes unrelated to tumor or therapy were eliminated from the analysis. Tumor volume was calculated as $x^2y / 2$, where x = width, y = length, and $x < y$, and was reported as the mean and SD values obtained from five FJ9-treated mice and four PBS-treated mice.

Statistical analysis. A one-tailed Student's *t* test was used to compare the effect of treatment with that of no treatment (Fig. 3*B* and Fig. 4*B*).

Results

We conducted AlphaScreen energy transfer assays (33) that showed FJ9 to be a biochemical antagonist of the binding of Frz7 to DVL. The signal generated by the interaction of biotinylated Frz7 peptide and GST-fused human DVL PDZ domain was titrated with FJ9. As the concentration of FJ9 increased, the signal level dropped to that of the negative control, signifying competitive antagonism (Fig. 1*A*). The K_i value observed in this competitive assay was equivalent to the binding affinity of Frz7 (20) and Idax (34) peptides to the mDVL1. We confirmed that pretreatment with FJ9 for 30 min does not reduce the maximum signal intensity generated by the PDZ domain bound to Frz7 peptide. In addition, whereas the MAGI3 PDZ2 domain treated with the indole-3-carbinol compound shows a clear shift in mass spectrometry (29), the DVL3 PDZ domain exposed to FJ9 under identical conditions does not (data not shown). These data strongly suggest that FJ9 does not covalently bind to the DVL PDZ, at least within the period of observation. Although FJ9 was derived from a compound that binds to the MAGI3 PDZ2 domain, it inhibited DVL3 PDZ domain interactions >10 times as potently as MAGI3 PDZ2 interactions (Supplementary Fig. S2). To determine whether FJ9 would inhibit Frz7-DVL interaction in intact cells, we did a cellular coimmunoprecipitation analysis. HA-tagged mDVL1 and *myc*-tagged hFrz7 were transiently expressed in HEK293T cells. After cells were treated with FJ9, the DVL1-Frz7 complex was precipitated from the lysate with anti-HA agarose and analyzed by immunoblotting with an anti-*myc* antibody. FJ9 treatment diminished formation of the DVL1-Frz7 complex at concentrations above the *in vitro* K_i (Fig. 1*B*). Therefore, FJ9 penetrates the cell membrane and disrupts intracellular DVL1-Frz7 binding.

To compare the binding of FJ9 and the binding of native ligands to the DVL PDZ domain, we used the $^1H/^{15}N$ heteronuclear single-quantum coherence NMR method previously used to observe the binding of the mDVL1 PDZ domain to peptide ligands (20, 24, 34). Addition of FJ9 clearly shifted several peaks of the PDZ domain spectrum. The data in titration experiment shows that the PDZ domain and FJ9 are in fast exchange because peaks are shifted gradually with increasing concentrations of FJ9 (Fig. 2). The residues whose resonance peaks were shifted are located in the regions of the αB helix and the βB sheet that form the ligand-binding groove of the PDZ domain and are the residues perturbed by binding of the Frz7 peptide (20). However, unlike the Frz7 peptide, FJ9 caused no shifts in the region of the αA helix located

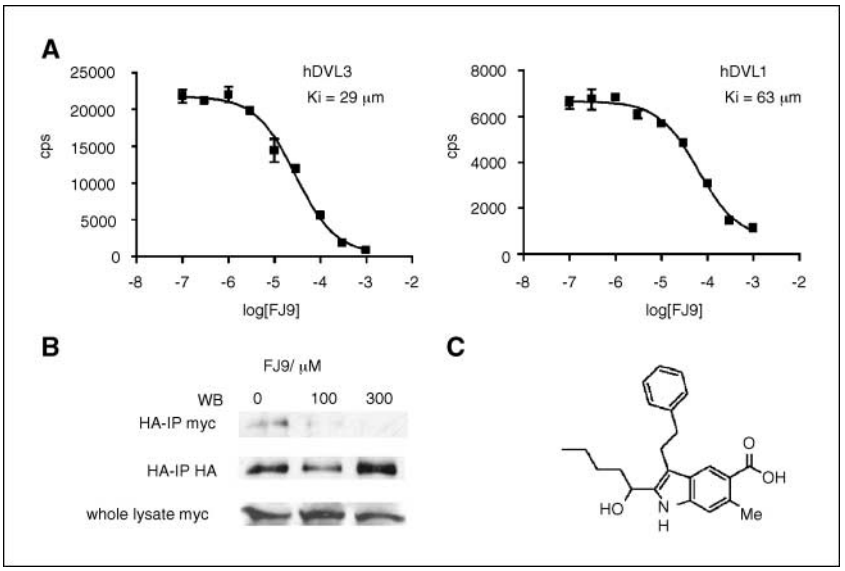

Figure 1. FJ9 disrupts protein-protein interaction between Frz7 and the PDZ domain of DVL. *A,* FJ9 exerts competitive antagonism against the binding of Frz7 peptide (10 μmol/L) to the PDZ domain (100 nmol/L) of hDVL1 (*left*) and hDVL3 (*right*). *Points,* mean; *bars,* SD. *B,* inhibition of complex formation between HA-tagged DVL1 and *myc*-tagged Frz7 in intact HEK293T cells treated with FJ9. *C,* chemical structure of FJ9.

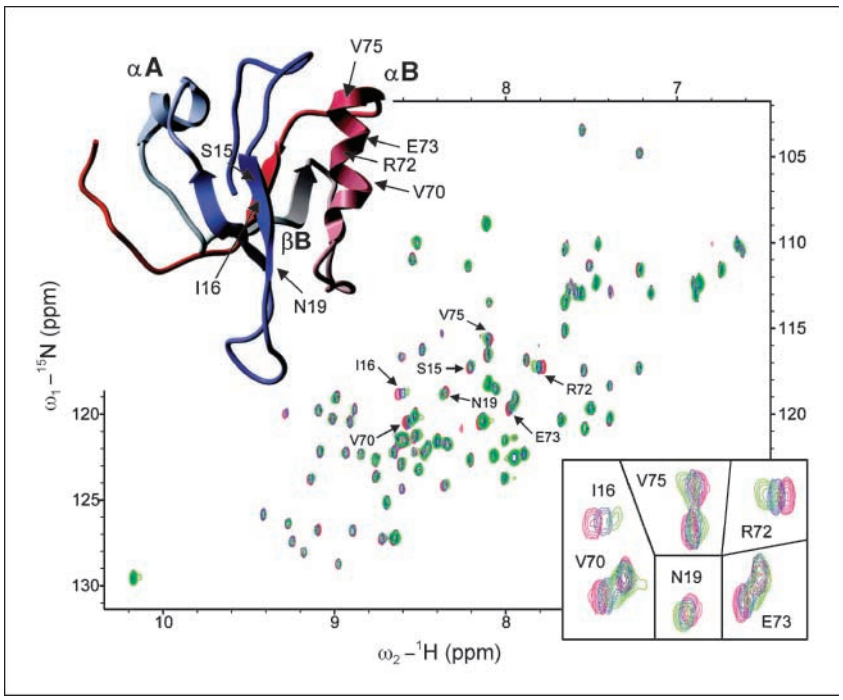

Figure 2. Chemical shift perturbation of the mouse DVL1 PDZ domain after treatment with FJ9. *Red,* $^1H/^{15}N$ heteronuclear single-quantum coherence NMR spectrum for free PDZ domain; *blue,* PDZ domain with 3 equivalents of FJ9; *green,* PDZ domain with 10 equivalents of FJ9. Peaks corresponding to residue Ser^{15}, I16, N19, V70, Arg^{72}, E73, and Val^{75} shifted when FJ9 was added to the protein. Shifted residues are shown on the ribbon representation of mDVL1 PDZ domain.

outside of the groove probably because of the relative compactness of FJ9. FJ9 caused smaller shifts than did Frz7 peptide, suggesting that FJ9 causes less conformational perturbation in the PDZ domain backbone.

To investigate whether FJ9 inhibits the Wnt signaling cascade, we assayed Wnt signaling in cells that had been treated with FJ9. DVL mediates at least two (i.e., canonical and non-canonical) Wnt signaling cascades (35). The canonical pathway is triggered by nuclear translocation of β-catenin followed by activation of Tcf transcription. To confirm if FJ9 inhibits the nuclear translocation of β-catenin DVL dependently, we used the well-characterized normal human mesothelial cell line LP9. LP9 has a stable growth control system, has no apparent tumorigenic potential (36), and shows only trace Wnt signaling (32), suggesting that the pathway is essentially dormant. We created LP9 cell lines stably expressing empty vector (mDVL1) or mDVL1 lacking the PDZ domain (ΔPDZ-DVL1; ref. 22). We hypothesized that if FJ9 acts by a DVL-specific mechanism, it would down-regulate cytosolic β-catenin only in the DVL1 cell line. After treatment with FJ9, we observed no significant cell death or morphologic change in any of the cell lines. However, cytosolic β-catenin was significantly down-regulated in a dose-dependent manner only in the DVL1 cells (Fig. 3*A*). These results suggest that FJ9 down-regulates the nuclear translocation of β-catenin by interacting directly with the DVL PDZ. Therefore, we expected that FJ9 down-regulates Tcf transcription regardless of β-catenin mutation. To confirm this hypothesis, we analyzed Tcf transcription activity in HCT116 cells in which Tcf signaling is constitutively activated because of mutated gene encoding non-degradative β-catenin (37). At concentrations above the antagonism K_i (Fig. 1*A*), FJ9 inhibited Tcf promoter activity dose-dependently, as measured by a TCF optimal promoter (TOPflash) reporter assay (37), but had less effect on the negative mutant control reporter FOPflash (Fig. 3*B*). The Tcf transcription up-regulates several gene products involved in mitosis, including *c-myc* (38), *cyclin D1* (39), and *survivin* (40). Consistently, Western blot analysis revealed that FJ9 significantly down-regulates these canonical Wnt signaling molecules (Fig. 3*C* and *E*). Down-regulation of the signaling was confirmed at the mRNA level. FJ9 suppressed survivin and cyclin D1 mRNA in this cell with a dose dependency similar to that observed at the protein level (Fig. 3*D* and *F*). Suppression of Wnt signaling by silencing the *DVL* gene (23) also down-regulated the *survivin* gene (Fig. 3*F*). Taken together, these results suggest that FJ9 inhibits the Tcf transcriptional activity by directly suppressing DVL-mediated nuclear translocation of β-catenin.

DVL is a weak activator of Akt (41), and FJ9 slightly reduced the level of activated Akt as well (Fig. 3*C*). The DVL PDZ domain is not essential for activation of the JNK, a key mediator of non-canonical Wnt signaling (42). FJ9 had no effect on JNK activity in HeLa cells transfected with mDVL1 (Fig. 3*G*). Because JNK activation exerts a proapoptotic stimulus (43), we hypothesized that FJ9 would fail to induce apoptosis in the absence of β-catenin signaling. To test this hypothesis, we observed the effect of FJ9 on H28 mesothelioma cells expressing high levels of Wnt1 but containing a homozygous deletion of the *β-catenin* gene (13, 44). FJ9 neither suppressed growth nor induced apoptosis (Fig. 4*A*). This result differs strikingly from the JNK-dependent apoptosis of H28 cells observed when Wnt-Frz interaction is inhibited by Wnt1 siRNA (13), Dickkopf-1 (45), or sFRP4 (46). These results suggest that the cellular effect of FJ9 is independent of the JNK-mediated pathway. This finding is also consistent with the weak binding affinity of FJ9 for MAGI3 (Supplementary Fig. S2), which regulates JNK activation through binding with Frz4 (47). To further investigate if FJ9 perturb other signaling than the Wnt pathway, we observed the effect of FJ9 on total gene expression. HCT116 cells were treated with FJ9 under a concentration in which their Tcf activity is only modestly diminished (100 μmol/L), and their RNA was analyzed by using Affymetrix GeneChips. Only 0.8% of probe sets were either up-regulated or down-regulated >2-fold (Supplementary Fig. S3).

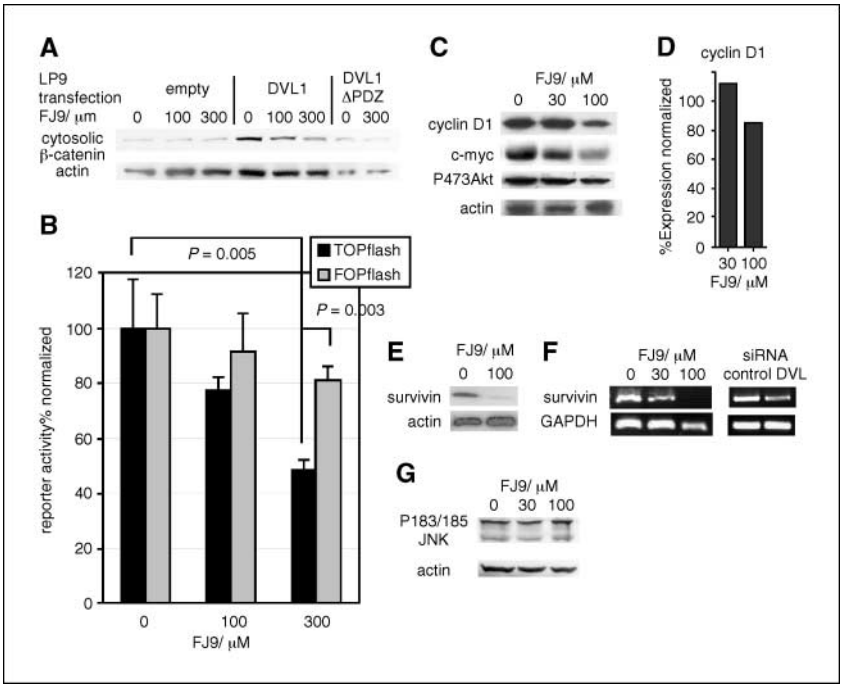

Figure 3. FJ9 inhibits the canonical Wnt signaling pathway. *A,* down-regulation of cytosolic β-catenin in *hTERT*-immortalized LP9 cells stably expressing the indicated vectors after a 2-day treatment with FJ9. The cells retained normal growth and differentiation. *B,* normalized TOPflash and FOPflash reporter luciferase activity in HCT116 p53$^{-/-}$ cells treated with FJ9 for 1 day. *Columns,* mean; *bars,* SD. *C,* down-regulation of canonical Wnt signaling molecules in HCT116 cells after 2 days of FJ9 treatment. *D,* Taqman analysis of cyclin D1 mRNA in HCT116 cells after FJ9 treatment for 1 day. *E,* down-regulation of survivin in H1703 cells after FJ9 treatment for 1 day. *F,* RT-PCR analysis of survivin mRNA in HCT116 cells after treatment with FJ9 for 1 day (*left*) or DVL siRNA for 2 days (*right*). *G,* FJ9 treatment for 1 day did not affect JNK dual phosphorylation in mDVL1-transfected HeLa cells.

Taken together, these results suggest that effect of FJ9 is specific to DVL PDZ domain but not perturbing diverse cell signaling promiscuously.

We next investigated the effect of FJ9 on the growth of tumor cells with intact β-catenin signaling. In the LOX melanoma cell line and the H460 and H1703 non–small cell lung cancer cell lines, FJ9 caused significant apoptosis at the same concentrations at which it suppressed Tcf promoter activity (Fig. 4*A*). In contrast, FJ9 had little discernible effect on primary cultures of NHBE cells or SAEC, neither of which expresses Wnt-1. These results show that the absence of Wnt-1 in normal tissues (32) accounts for the tumor-specific effect of FJ9. To assess the therapeutic potential of FJ9 *in vivo*, we measured inhibition of tumor growth by FJ9 in a mouse xenograft model. H460 cells were transplanted into nude mice to induce tumors. Daily administration of FJ9 began after 7 days and continued for 14 days. FJ9 significantly inhibited the growth of the tumor xenografts (Fig. 4*B*). The mice showed no significant weight loss (<5%; data not shown).

Discussion

This study was based on the hypothesis that activation of the upstream Wnt pathway is an important contributor to diverse human cancers. Overexpression of Frz7 and DVL3 has been suggested to play a causative role in human carcinogenesis. Consistent with this observation, we have shown that an inhibitor of Frz7-DVL3 interaction selectively down-regulates canonical Wnt signaling via suppression of β-catenin nuclear translocation. Cancer stem cell signalings, such as Wnt and Hedgehog pathways, are connected by protein-protein interaction network rather than enzymatic signaling events. Therefore, small-molecule drugs that antagonize protein-protein interactions in those signaling pathways show promise as the next generation of antitumor agents. There has been more enthusiasm for traditional enzyme inhibitors (e.g., kinase inhibitors and protease inhibitors) than for protein-protein interaction antagonists for tumor therapies. However, several recent studies clearly show the therapeutic usefulness of protein-protein interaction antagonists, such as antagonists of

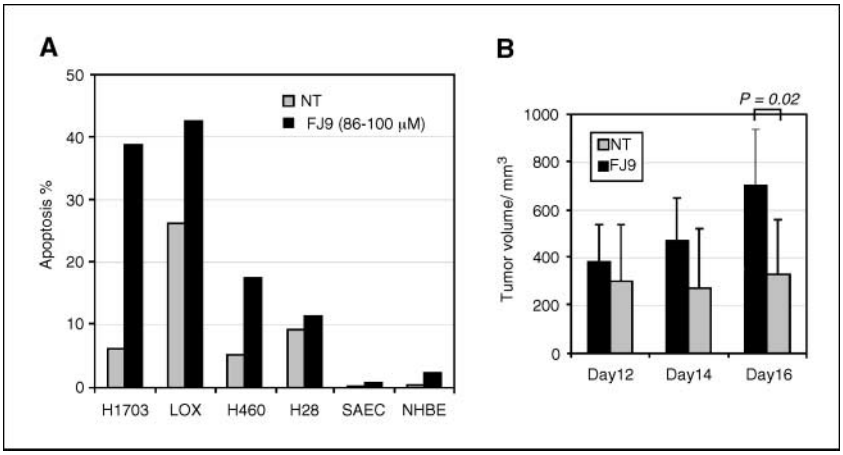

Figure 4. FJ9 suppresses the growth of tumor cells in a β-catenin–dependent manner. *A,* flow cytometric analysis of Annexin V in treated cells. LOX and H460, 86 μmol/L (3 days); H28, 100 μmol/L (3 days); H1703, 100 μmol/L (4 days); SAEC and NHBE, 100 μmol/L (6 days). *B,* one week after s.c. injection of H460 tumor cells, nude mice began receiving daily i.p. injections of FJ9 (50 mg/kg = 137 μmol/L) or PBS. Tumor size and body weight (data not shown) were measured on days 12, 14, and 16 after the start of treatment. *NT,* not treated (PBS). *Columns,* mean; *bars,* SD.

MDM2 (48) and Smoothened (49). In this study, we have shown that a new small-molecule antagonist of DVL suppresses tumor growth.

One concern associated with small-molecule drugs is specificity. We have shown that FJ9 causes little effect on global gene expression (Supplementary Fig. S3). The cellular effect of FJ9 is well correlated with its PDZ domain antagonism activity. For example, the effects of FJ9 on cell signaling are subtle at 30 μmol/L but significant at 100 μmol/L (Fig. 3), consistent with its antagonism K_i (Fig. 1*A*). Furthermore, our data suggest that FJ9 may have little effect on the non-canonical Wnt pathway, as the phosphorylated JNK level remained unchanged after FJ9 treatment (Fig. 3*G*), although we can not completely rule out the possibility of involvement of the non-canonical pathway. The specificity of FJ9 is further supported by the fact that FJ9 had minimal effect on a mesothelioma cell line with homozygous deletion of the *β-catenin* gene and on normal cells even at 100 μmol/L (Fig. 4*A*). Taken together, the evidence suggests that the cellular effects of FJ9 are based on DVL PDZ domain antagonism but not on promiscuous pharmacologic effects. The specificity of FJ9 to DVL PDZ is also supported by our finding that FJ9 decreased the level of cytosolic β-catenin only in LP9 cells stably transfected with DVL, not in control and ΔPDZ-DVL LP9 cell lines (Fig. 3*A*).

Previously, we proved the hypothesis that DVL overexpression is critical to Wnt signaling activation in lung cancer and prevalent as a result of activated upstream signaling (22, 23). The apoptotic effect of FJ9 in lung cancer cells correlates with our previous findings that both DVL siRNA and dominant-negative ΔPDZ-DVL decreased cytosolic β-catenin levels and diminished Tcf-mediated transcription in human mesothelioma cells. Survivin is down-regulated by either FJ9 or DVL siRNA treatment (Fig. 3*E* and *F*). Because inhibition of survivin expression is sufficient to cause apoptosis and synergize with chemotherapy in human cancer cells (50), FJ9 may have a synergistic effect on these cancer cells when combined with cytotoxic chemotherapy.

In summary, our study indicates that small-molecule antagonists of PDZ domain interaction of DVL can down-regulate the β-catenin–dependent Wnt signaling pathway and induce apoptosis in human lung cancer and melanoma cells. These findings support the further development of this potential strategy for the treatment of cancer. Additional studies to find more efficient compounds for clinical usefulness are now under way.

Acknowledgments

Received 7/24/2006; revised 9/27/2006; accepted 11/7/2006.

Grant support: Sandler Research Foundation (N. Fujii and R.K. Guy), Sidney Kimmel Research Foundation (N. Fujii and R.K. Guy), American Lebanese Syrian Associated Charities (N. Fujii, R.K. Guy, J. Shan, G. Neale, and J. Zheng), NIH grant RO1 CA 093708-01A3, Larry Hall and Zygielbaum Memorial Trust, and Kazan, McClain, Edises, Abrams, Fernandez, Lyons, and Farrise Foundation (L. You, Z. Xu, B. He, I. Mikami, Y. Shi, and D.M. Jablons).

The costs of publication of this article were defrayed in part by the payment of page charges. This article must therefore be hereby marked *advertisement* in accordance with 18 U.S.C. Section 1734 solely to indicate this fact.

We thank Kiran Kodali for protein mass spectrometry, Yihui Shi for RNA isolation, and Sharon Naron (St. Jude Children's Research Hospital) and Richard N. Barg (University of California, San Francisco) for editorial advice of this article.

References

1. Polakis P. Wnt signaling and cancer. Genes Dev 2000;14:1837–51.
2. Moon RT, Kohn AD, De Ferrari GV, et al. WNT and β-catenin signalling: diseases and therapies. Nat Rev Genet 2004;5:691–701.
3. Reya T, Clevers H. Wnt signalling in stem cells and cancer. Nature 2005;434:843–50.
4. Mazieres J, You L, He B, et al. Inhibition of Wnt16 in human acute lymphoblastoid leukemia cells containing the t(1;19) translocation induces apoptosis. Oncogene 2005;24:5396–400.
5. Casagrande G, te Kronnie G, Basso G. The effects of siRNA-mediated inhibition of E2A-PBX1 on EB-1 and Wnt16b expression in the 697 pre-B leukemia cell line. Haematologica 2006;91:765–71.
6. Calvo R, West J, Franklin W, et al. Altered HOX and WNT7A expression in human lung cancer. Proc Natl Acad Sci U S A 2000;97:12776–81.
7. Ohira T, Gemmill RM, Ferguson K, et al. WNT7a induces E-cadherin in lung cancer cells. Proc Natl Acad Sci U S A 2003;100:10429–34.
8. Winn RA, Marek L, Han SY, et al. Restoration of Wnt-7a expression reverses non-small cell lung cancer cellular transformation through frizzled-9-mediated growth inhibition and promotion of cell differentiation. J Biol Chem 2005;280:19625–34.
9. Bremnes RM, Veve R, Gabrielson E, et al. High-throughput tissue microarray analysis used to evaluate biology and prognostic significance of the E-cadherin pathway in non-small-cell lung cancer. J Clin Oncol 2002;20:2417–28.
10. Hommura F, Furuuchi K, Yamazaki K, et al. Increased expression of β-catenin predicts better prognosis in nonsmall cell lung carcinomas. Cancer 2002;94:752–8.
11. Retera JM, Leers MP, Sulzer MA, et al. The expression of β-catenin in non-small-cell lung cancer: a clinicopathological study. J Clin Pathol 1998;51:891–4.
12. Awaya H, Takeshima Y, Amatya VJ, et al. Loss of expression of E-cadherin and β-catenin is associated with progression of pulmonary adenocarcinoma. Pathol Int 2005;55:14–8.
13. You L, He B, Uematsu K, et al. Inhibition of Wnt-1 signaling induces apoptosis in β-catenin-deficient mesothelioma cells. Cancer Res 2004;64:3474–8.
14. Liu T, DeCostanzo AJ, Liu X, et al. G protein signaling from activated rat frizzled-1 to the β-catenin-Lef-Tcf pathway. Science 2001;292:1718–22.
15. Caricasole A, Ferraro T, Iacovelli L, et al. Functional characterization of WNT7A signaling in PC12 cells: interaction with A FZD5 x LRP6 receptor complex and modulation by Dickkopf proteins. J Biol Chem 2003;278:37024–31.
16. Merle P, Kim M, Herrmann M, et al. Oncogenic role of the frizzled-7/β-catenin pathway in hepatocellular carcinoma. J Hepatol 2005;43:854–62.
17. Vincan E, Darcy PK, Smyth MJ, et al. Frizzled-7 receptor ectodomain expression in a colon cancer cell line induces morphological change and attenuates tumor growth. Differentiation 2005;73:142–53.
18. Sagara N, Toda G, Hirai M, et al. Molecular cloning, differential expression, and chromosomal localization of human frizzled-1, frizzled-2, and frizzled-7. Biochem Biophys Res Commun 1998;252:117–22.
19. Tanaka S, Akiyoshi T, Mori M, et al. A novel frizzled gene identified in human esophageal carcinoma mediates APC/β-catenin signals. Proc Natl Acad Sci U S A 1998;95:10164–9.
20. Wong HC, Bourdelas A, Krauss A, et al. Direct binding of the PDZ domain of Dishevelled to a conserved internal sequence in the C-terminal region of Frizzled. Mol Cell 2003;12:1251–60.
21. Bui TD, Beier DR, Jonssen M, et al. cDNA cloning of a human dishevelled DVL-3 gene, mapping to 3q27, and expression in human breast and colon carcinomas. Biochem Biophys Res Commun 1997;239:510–6.
22. Uematsu K, Kanazawa S, You L, et al. Wnt pathway activation in mesothelioma: evidence of Dishevelled overexpression and transcriptional activity of β-catenin. Cancer Res 2003;63:4547–51.
23. Uematsu K, He B, You L, et al. Activation of the Wnt pathway in non small cell lung cancer: evidence of dishevelled overexpression. Oncogene 2003;22:7218–21.
24. Shan J, Shi DL, Wang J, et al. Identification of a specific inhibitor of the Dishevelled PDZ domain. Biochemistry 2005;44:15495–503.
25. Sheng M, Sala C. PDZ domains and the organization of supramolecular complexes. Annu Rev Neurosci 2001;24:1–29.
26. Harris BZ, Lim WA. Mechanism and role of PDZ domains in signaling complex assembly. J Cell Sci 2001;114:3219–31.
27. Aarts M, Liu Y, Liu L, et al. Treatment of ischemic brain damage by perturbing NMDA receptor-PSD-95 protein interactions. Science 2002;298:846–50.
28. Dev KK. Making protein interactions druggable: targeting PDZ domains. Nat Rev Drug Discov 2004;3:1047–56.
29. Fujii N, Haresco JJ, Novak KA, et al. A selective irreversible inhibitor targeting a PDZ protein interaction domain. J Am Chem Soc 2003;125:12074–5.
30. Dickson MA, Hahn WC, Ino Y, et al. Human keratinocytes that express hTERT and also bypass a p16(INK4a)-enforced mechanism that limits life span become immortal yet retain normal growth and differentiation characteristics. Mol Cell Biol 2000;20:1436–47.
31. Wang CY, Guttridge DC, Mayo MW, et al. NF-κB induces expression of the Bcl-2 homologue A1/Bfl-1 to preferentially suppress chemotherapy-induced apoptosis. Mol Cell Biol 1999;19:5923–9.
32. He B, You L, Uematsu K, et al. A monoclonal antibody against Wnt-1 induces apoptosis in human cancer cells. Neoplasia 2004;6:7–14.
33. Wilson J, Rossi CP, Carboni S, et al. A homogeneous 384-well high-throughput binding assay for a TNF receptor using alphascreen technology. J Biomol Screen 2003;8:522–32.

34. London TB, Lee HJ, Shao Y, et al. Interaction between the internal motif KTXXXI of Idax and mDvl PDZ domain. Biochem Biophys Res Commun 2004;322:326–32.

35. Wharton KA, Jr. Runnin' with the Dvl: proteins that associate with Dsh/Dvl and their significance to Wnt signal transduction. Dev Biol 2003;253:1–17.

36. Connell ND, Rheinwald JG. Regulation of the cytoskeleton in mesothelial cells: reversible loss of keratin and increase in vimentin during rapid growth in culture. Cell 1983;34:245–53.

37. Korinek V, Barker N, Morin PJ, et al. Constitutive transcriptional activation by a β-catenin-Tcf complex in $APC^{-/-}$ colon carcinoma. Science 1997;275:1784–7.

38. He TC, Sparks AB, Rago C, et al. Identification of c-MYC as a target of the APC pathway. Science 1998;281:1509–12.

39. Tetsu O, McCormick F. β-Catenin regulates expression of cyclin D1 in colon carcinoma cells. Nature 1999;398:422–6.

40. Kim PJ, Plescia J, Clevers H, et al. Survivin and molecular pathogenesis of colorectal cancer. Lancet 2003;362:205–9.

41. Fukumoto S, Hsieh CM, Maemura K, et al. Akt participation in the Wnt signaling pathway through Dishevelled. J Biol Chem 2001;276:17479–83.

42. Li L, Yuan H, Xie W, et al. Dishevelled proteins lead to two signaling pathways. Regulation of LEF-1 and c-Jun N-terminal kinase in mammalian cells. J Biol Chem 1999;274:129–34.

43. Liu J, Lin A. Role of JNK activation in apoptosis: a double-edged sword. Cell Res 2005;15:36–42.

44. Usami N, Sekido Y, Maeda O, et al. β-Catenin inhibits cell growth of a malignant mesothelioma cell line, NCI-H28, with a 3p21.3 homozygous deletion. Oncogene 2003;22:7923–30.

45. Lee AY, He B, You L, et al. Dickkopf-1 antagonizes Wnt signaling independent of β-catenin in human mesothelioma. Biochem Biophys Res Commun 2004;323:1246–50.

46. He B, Lee AY, Dadfarmay S, et al. Secreted frizzled-related protein 4 is silenced by hypermethylation and induces apoptosis in β-catenin-deficient human mesothelioma cells. Cancer Res 2005;65:743–8.

47. Yao R, Natsume Y, Noda T. MAGI-3 is involved in the regulation of the JNK signaling pathway as a scaffold protein for frizzled and Ltap. Oncogene 2004;23:6023–30.

48. Tovar C, Rosinski J, Filipovic Z, et al. Small-molecule MDM2 antagonists reveal aberrant p53 signaling in cancer: implications for therapy. Proc Natl Acad Sci U S A 2006;103:1888–93.

49. Romer JT, Kimura H, Magdaleno S, et al. Suppression of the Shh pathway using a small molecule inhibitor eliminates medulloblastoma in Ptc1(+/−)p53(−/−) mice. Cancer Cell 2004;6:229–40.

50. Grossman D, Altieri DC. Drug resistance in melanoma: mechanisms, apoptosis, and new potential therapeutic targets. Cancer Metastasis Rev 2001;20:3–11.

Correction: Antagonist of Dishevelled Suppressing Tumor Cell Growth

In the article on antagonist of Dishevelled suppressing tumor cell growth in the January 15, 2007 issue of *Cancer Research* (1), there is an error in Fig. 4*B*; the labels for NT and FJ9 were switched. The corrected figure appears below.

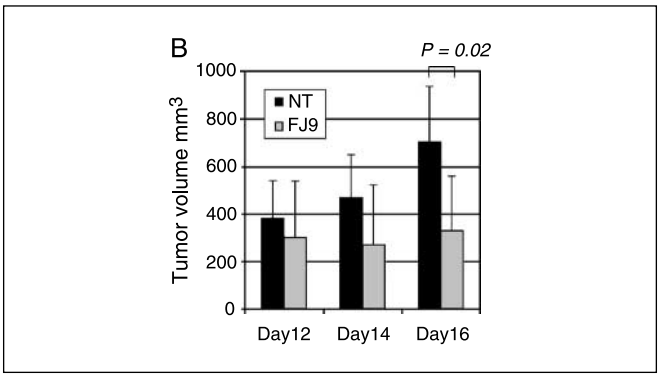

1. Fujii N, You L, Xu Z, Uematsu K, Shan J, He B, Mikami I, Edmondson LR, Neale G, Zheng J, Guy RK, Jablons DM. An antagonist of Dishevelled protein-protein interaction suppresses β-catenin–dependent tumor cell growth. Cancer Res 2007; 67:573–9.

doi:10.1158/0008-5472.CAN-67-5-COR2

An Antagonist of Dishevelled Protein-Protein Interaction Suppresses β-Catenin–Dependent Tumor Cell Growth

Naoaki Fujii, Liang You, Zhidong Xu, et al.

Cancer Res 2007;67:573-579.